Influence of First Stage Mass Variation on Satellite-Launch Vehicle Longitudinal Vibrations

Augusto Molica Silva Guimarães[1], Carlos d'Andrade Souto[2]

[1]PG-CTE, Technological Institute of Aeronautics
Praça Marechal Eduardo Gomes, 50, 12228-900, São José dos Campos/SP, Brazil
augusto.molica@gmail.com
[2]Division of Integration and Tests, Institute of Aeronautics and Space
Praça Marechal Eduardo Gomes, 50, 12228-900, São José dos Campos/SP, Brazil
carlos.dandrade.souto@gmail.com

Abstract. During the launch phase, satellites are subjected to intense dynamic loads. Part of these loads is due to acoustic excitation from the exhaust jet stream and other aerodynamic effects and part is due to different phenomena that originate in the launch vehicle propulsive system. The later can cause vibrations that propagate longitudinally along the rocket structure and can reach the satellite. This paper analyzes the influence of the effect of mass variation of the first stage of a launch vehicle in the longitudinal dynamic response of its payload during lift-off and the first phase of the flight. A discrete multi degree of freedom model was implemented to evaluate the longitudinal vibrations of a real launcher-satellite set when subjected to thrust oscillations.

Keywords: vibrations, launch vehicle, dynamic loads, mass variation, thrust oscillation.

1 Introduction

Satellites go under high dynamic loading during the launch vehicle flight due to acoustic, aerodynamic and structural forces (Liu et al [1]). During liftoff, the most intense dynamic loads have an acoustic origin (Pirk et al [2]). These loads act predominantly in transverse directions to the longitudinal axis of the launch vehicle. Longitudinal dynamic loads originate mainly from the launcher's propulsive system. Thrust oscillations often occur in solid propellant rocket engines (Fabignon et al [3]) and can generate dynamic longitudinal loads in a launch vehicle. These loads can reach the payload and generate structural vibrations in the satellite. Take this into account allow engineers to design satellites strong enough to bear these loads and payload attach fairings that mitigate the vibrations the payload undergoes. As shown in Guimarães and Souto [4], considering the launch vehicle as a single rigid body can lead, in some cases, to errors in evaluating longitudinal vibrations.

By analyzing a 4 degree of freedom mass-spring-damper model of a three-staged launch vehicle with a satellite, this paper aims to study the influence of 1st stage mass variation on the satellite's dynamic response to launcher longitudinal vibrations caused by thrust oscillations. The stage masses considered correspond to the stage masses of the Arianespace Vega launcher [5]. The stiffness values of the interstage structures were obtained from Jafari [6] and Karahalis [7].

2 Theory

The matrix differential equation that models the dynamic behavior of a discrete mechanical system is shown in eq. (1), where [M], [C] and [K] are, respectively, the mass, damping and stiffness matrices; $\{x\}$, $\{\dot{x}\}$ and $\{\ddot{x}\}$ are the masses' displacement vector and its first and second derivatives with respect to time respectively; and $\{F\}$ is the force vector.

$$[M]\{\ddot{x}\} + [C]\{\dot{x}\} + [K]\{x\} = \{F\} \tag{1}$$

For this analysis, we are considering the satellite and launch vehicle system as the model shown in Fig. 1. All displacements, velocities and accelerations are referred to an inertial system fixed to the ground. In this work the actual Vega launcher's 4th stage was considered rigidly attached to the adapter and both treated as a single structural element connecting the 3rd stage (m_3) to the satellite (m_s).

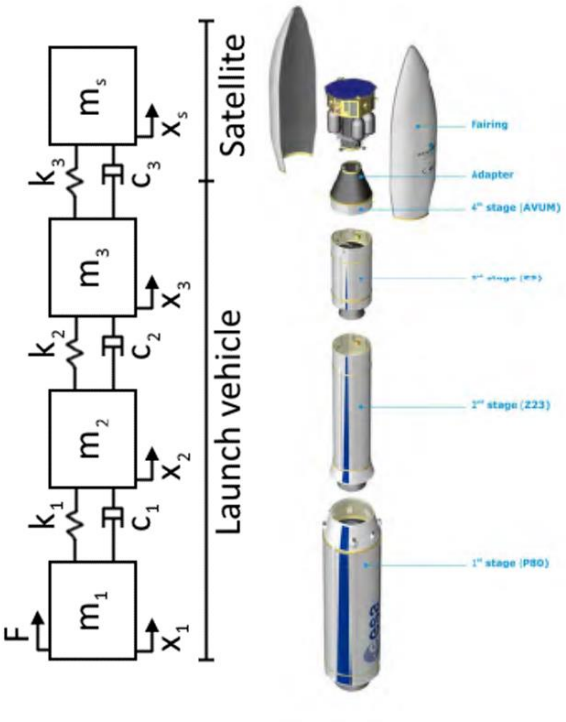

Figure 1. Model of the launch vehicle and satellite system (adapted from [5])

The matrices and vectors for this model are shown in eq. (2).

$$[M] = \begin{bmatrix} m_1 & 0 & 0 & 0 \\ 0 & m_2 & 0 & 0 \\ 0 & 0 & m_3 & 0 \\ 0 & 0 & 0 & m_s \end{bmatrix}; [C] = \begin{bmatrix} c_1 & -c_1 & 0 & 0 \\ -c_1 & c_1 + c_2 & -c_2 & 0 \\ 0 & -c_2 & c_2 + c_3 & -c_3 \\ 0 & 0 & -c_3 & c_3 \end{bmatrix};$$
$$[K] \begin{bmatrix} k_1 & -k_1 & 0 & 0 \\ -k_1 & k_1 + k_2 & -k_2 & 0 \\ 0 & -k_2 & k_2 + k_3 & -k_3 \\ 0 & 0 & -k_3 & k_3 \end{bmatrix}; \{x\} = \begin{bmatrix} x_1 \\ x_2 \\ x_3 \\ x_s \end{bmatrix}; \{F\} = \begin{bmatrix} F \\ 0 \\ 0 \\ 0 \end{bmatrix} \tag{2}$$

The damping coefficients can be determined by the eq. (3), where $\boldsymbol{\zeta_i}$ is the damping ratio and $i = 1,2,3$.

$$c_i = 2\zeta_i\sqrt{m_i k_i} \tag{3}$$

The force F applied to mass m_1 is the thrust generated by the P80 motor. During engine burnout, the thrust amplitude varies relatively smoothly, but it is common for oscillations in the thrust amplitude to occur especially

at the beginning and end of the burn [8]. Figure 2, taken from Zhang, Q., et al [9], shows the thrust curve with amplitude oscillations of a solid propellant rocket engine obtained from fluid dynamics studies.

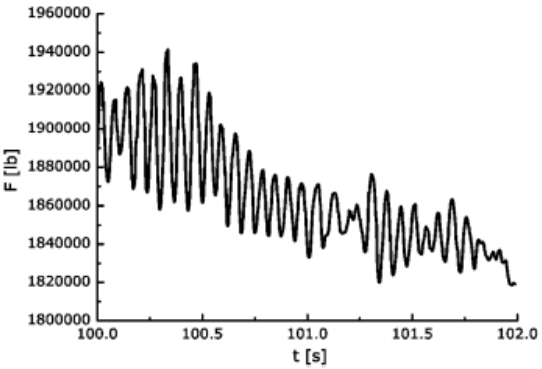

Figure 2 Thrust oscillations (extracted from [9])

Thrust oscillations can be caused by the interaction between longitudinal acoustic modes of the engine tube, and the burning process inside the engine as pointed out by Zhang, Q., et al [9]. In this work we consider that the oscillation of the 1st stage thrust is caused by the interaction of the burning with the 1st longitudinal acoustic mode of the rocket engine. The thrust perturbation was considered as a sinusoidal oscillation tunned to this frequency and with 1000 N of amplitude**.**

A solid propellant rocket engine has a closed end and an open end (the nozzle). However, in the divergent of the nozzle, the gas flow velocity becomes supersonic, and from an acoustic point of view, this region behaves like a rigid wall reflecting the sound waves Laudien [10]. Therefore, to calculate the natural frequency of the 1st longitudinal mode of the rocket engine, it must be considered a tube closed at both ends. According to Blevins and Plunkett [11], the frequency of the first longitudinal acoustic mode of a closed tube is presented in eq. (4), where $\boldsymbol{L}$ is the length of the cavity and $\boldsymbol{c}$ is the sound speed.

$$f_1 = \frac{c}{2L} \tag{4}$$

To estimate the satellite (m_s) acceleration response to a harmonic force applied to the 1st stage (m_1) both force and displacement are considered varying harmonically and so the discrete system displacement and force nodal vectors can be written as displayed in eq. (5) where $\{\bar{X}\}$ and $\{\bar{F}\}$ are the amplitudes vectors of the displacement and force, respectively, and ω is the angular frequency of the harmonic force [12]. By combining eqs. (5) and (1) and differentiating with respect to time twice one obtains the acceleration response showed in eq. (6).

$$\begin{cases} \{x\} = \{\bar{X}\}\exp(j\omega t) \\ \{F\} = \{\bar{F}\}\exp(j\omega t) \end{cases} \tag{5}$$

$$\{\ddot{x}\} = -\omega^2(-\omega^2[M] + j\omega[C] + [K])^{-1}\{F\} \tag{6}$$

To estimate the satellite acceleration response to a transient excitation applied to the 1st stage (the thrust), the Runge-Kutta fourth-order integration method was implemented to calculate two cases: a) first stage mass varying without rocket thrust (i.e. only the sinusoidal perturbation force history applied on the first stage); b) first stage mass varying with P80-FW SRM engine vacuum thrust added to the sinusoidal perturbation force history applied on the first stage. The first case was chosen to show whether harmonic and transient analysis results would agree when varying the first stage mass over time, while the second case would show whether using a real rocket thrust added to the same sinusoidal perturbation force changes the response on satellite.

The variable that is analyzed is the satellite's response acceleration $\ddot{x}_s$. The satellite acceleration response only to the sinusoidal perturbation was calculated as follows: a) the response to thrust + sinusoidal perturbation

was calculated; b) the response to sinusoidal perturbation was calculated; c) the response obtained in (a) was subtracted from that obtained in (b).

To put the steady-state solution in the transient response graphics, the code that runs the latter also outputs the first stage's mass at each moment, and thus allowing us to plot the expected steady-state response if the mass at each instant was kept constant.

3 Results and discussion

The properties of the satellite and the launch vehicle used can be found in Tab. 1.

Table 1. Values used in the simulation

Property	Value	Unit
$m_{1,initial}$	96243	Kg
$m_{1,final}$	8882	Kg
m_2	26300	Kg
m_3	12000	Kg
m_4	1228	Kg
k_1	4×10^8	N/m
k_2	1×10^8	N/m
k_3	3.8×10^7	N/m
ζ_1	0.32	-
ζ_2	0.32	-
ζ_3	0.015	-
$F_{perturbation}$	1000	N
Burn time	109.9	s

To get a broad view of the system's behavior, using the steady-state solution varying the input frequency and the first stage mass (range within the initial and final values), the Fig. 3 was generated and shows the acceleration on the satellite ($\ddot{x}_s$). The yellow color represents the mass near the initial values, and the purple represents the final masses, and it can be noticed that a lower the mass of the first stage always leads to a higher acceleration, which means that considering solely the initial mass can lead to an underestimation of the dynamic loads.

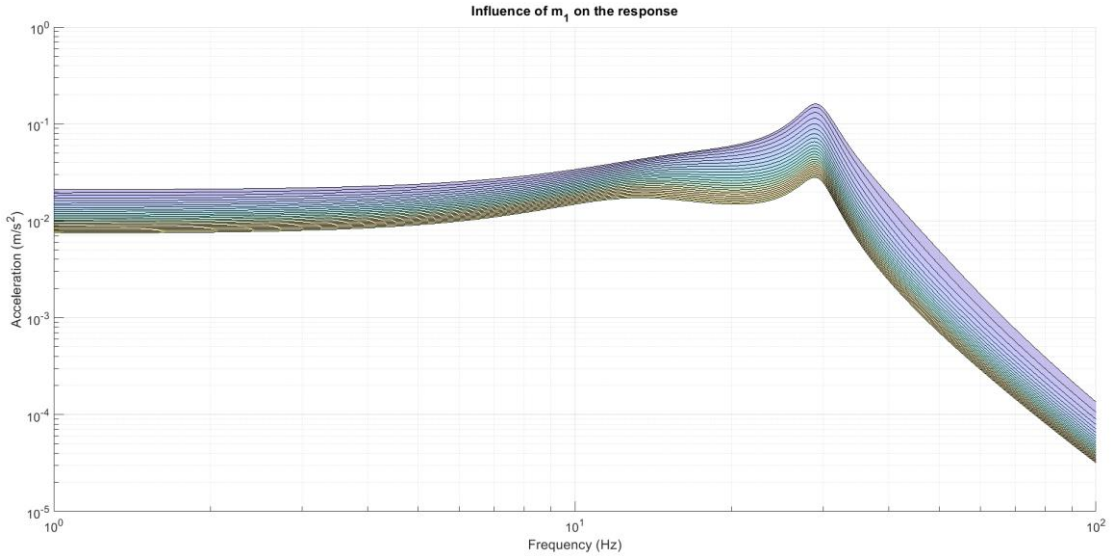

Figure 3. Influence of the first stage mass on the acceleration response

By using eq. (4) for $c = 1080\ m/s$ and $L = 11.2\ m$, we get a frequency of 48.2Hz, and thus this frequency was chosen to be used in the sinusoidal oscilation . The reponses for the three cases described above (steady-state and transient with and without the engine thrust), are plotted in Fig. 4.

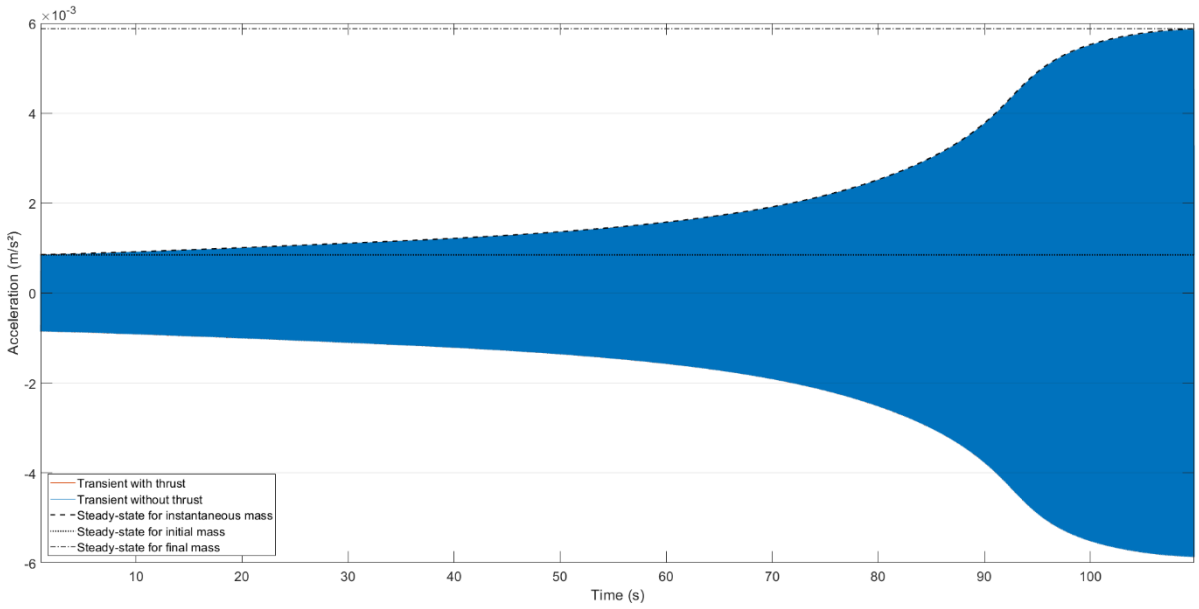

Figure 4. Response comparison for 48.2Hz perturbation

The "Transient with thrust" curve cannot be seen in Fig. 4 because the "Transient without thrust" curve superposes it, and using dashed lines did not help with the visualization. Since the selected frequency makes the payload oscilate thousands of times in the time span presented in Fig. 4, this plot's time span was narrowed to one second, between 90 and 91 seconds, to illustrate better the behavior of the system and to demostrate the aforementioned overlapped curve, and the Fig. 5 was generated.

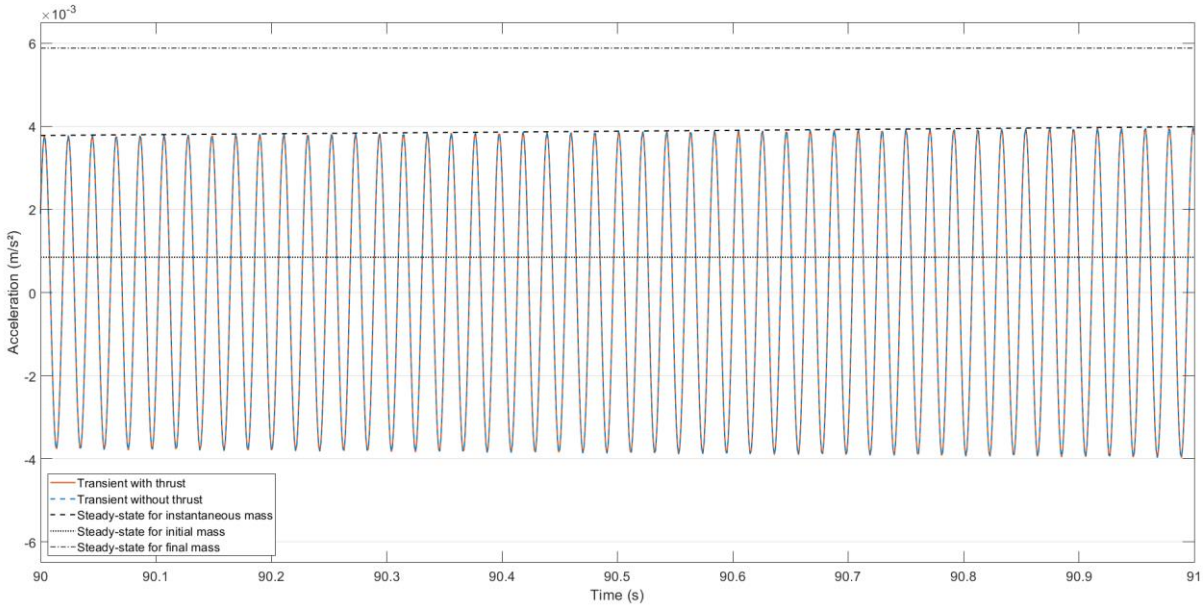

Figure 5. Response comparison for 48.2Hz perturbation (90 to 91 seconds)

By analyzing the Fig. 4, we can observe that: the steady-state for a constant initial mass is the lower bound of the acceleration amplitude, while using the final mass is a good estimation of the upper bound; the steady-state analysis present no noticeable difference when comparing to the transient curves; although this can't be seen in Fig. 4, both transient forces are coincident, which can be seen in Fig. 5.

4 Conclusions

When the mass of the first stage decreases over time, the amplitude of the vibrational loads on the satellite increases, and considering solely the initial mass can lead to an underestimation of the total loads, while considering the final mass give a reasonable result for the maximum load. By comparing the transient response and the steady-state response to the sinusoidal excitation only, we can conclude that, if only the amplitude of the acceleration at each moment is relevant, a steady-state solution calculated using the mass at each instant is a fair approximation to the transient response of this system with time varying mass. Regarding both transient responses, the results were coincident, which it is expected since the differential equation of the system is linear, and thus an analysis of the behavior changes due to periodic forces can be done separately from the quasi-static forces.

Acknowledgements. The authors thanks the support of '*Coordenação de Aperfeiçomento de Pessoal de Nível Superior'* (CAPES) for the PROAP support and for the scholarship granted to the first author.

Authorship statement. The authors hereby confirm that they are the sole liable persons responsible for the authorship of this work, and that all material that has been herein included as part of the present paper is either the property (and authorship) of the authors, or has the permission of the owners to be included here.

References

[1] Liu, L. K., et al. "Dynamic design of octostrut platform for launch stage whole-spacecraft vibration isolation." Journal of spacecraft and rockets 42.4 (2005): 654-662.
[2] Pirk, Rogério, et al. "Acoustics and Vibro-Acoustics Applied in Space Industry." Modeling and Measurement Methods for Acoustic Waves and for Acoustic Microdevices (2013): 479-512.
[3] Fabignon, Yves, et al. "Instabilities and pressure oscillations in solid rocket motors." Aerospace science and technology 7.3 (2003): 191-200.
[4] Guimarães, A.M.S.; Souto, C.A. "Influence of interstage damping on satellite-launch vehicle longitudinal vibrations." Journal of Research in Engineering and Applied Sciences, Vol. 06, Issue 02, April 2021.
[5] Arianespace Vega user's manual issue 4 revision 0, 2014
[6] Jafari, Behzad. WHOLE SPACECRAFT VIBRATION ISOLATION: A COMPARISON OF PASSIVE VS. SEMI-ACTIVE ISOLATION DESIGNS. Diss. Concordia University, 2018.
[7] Karahalis, Gregory G. *Whole Spacecraft Vibration Isolation* Diss. Air Force Institute of Technology, 1999
[8] Calvi, Adriano. "Spacecraft structural dynamics & loads an overview." Satellite Engineering Class (2010).
[9] Zhang, Q., Zhijun Wei, Wan-xing Su, Junwei Li and N. Wang. "Theoretical Modeling and Numerical Study for Thrust-Oscillation Characteristics in Solid Rocket Motors." *Journal of Propulsion and Power* 28 (2012): 312-322.
[10] Laudien, E., et al. "Experimental procedures aiding the design of acoustic cavities." Progress in Astronautics and Aeronautics 169 (1995): 377-402.
[11] Blevins, Robert D., and R. Plunkett. "Formulas for natural frequency and mode shape." Journal of Applied Mechanics 47.2 (1980): 461.
[12] Kelly, S. Graham. "Fundamentals of mechanical vibrations." (1992).